



1  
2  
3  
4  
5  
6  
7  
8  
9  
10  
11  
12  
13  
14  
15  
16  
17  
18  
19  
20  
21  
22  
23  
24  
25  
26  
27  
28  
29  
30  
31  
32  
33  
34  
35  
36  
37  
38  
39  
40  
41

## Geophysical and Geodetical Investigation of A Landslide Area (Koyulhisar-Sivas, Turkey)

Sevda ÖZEL<sup>1</sup>, Demet ÖVER<sup>2</sup> and Kemal Özgür HASTAOĞLU<sup>3</sup>

<sup>1,2</sup>Cumhuriyet University, Engineering Faculty, Department of Geophysical Engineering, 58140, Sivas, Turkey, [sozel@cumhuriyet.edu.tr](mailto:sozel@cumhuriyet.edu.tr).

<sup>3</sup>Cumhuriyet University, Engineering Faculty, Department of Geomatics Engineering, 58140, Sivas, Turkey, [khastaoglu@cumhuriyet.edu.tr](mailto:khastaoglu@cumhuriyet.edu.tr).

### Abstract

This study includes geophysical studies carried out in the last section in the close south of Koyulhisar (Sivas) landslide site. Additionally, the study area is in the most active location where landslide's displacement amount is the highest. The landslide site basically has been examined geophysics (SRT, GPR) and geodesic (GNSS) methods. According to the geophysical results, within ~20 m of investigation depth, layers with the average seismic P-wave velocities ( $V_p$ ) of 0.30, 1.00 and 2.00 km/s have been identified. It has been understood that the thickness of the first two layers of these layers from top to the bottom is approximately 3 and 6.5 m, and the last layer with  $V_p > 2.0$  km/s is the bedrock. Furthermore, it has been understood that the depth of the sliding surface which is the upper limit of the bedrock varies between ~7-10 m, there are loose units on the sliding surface, the type of sliding is planar sliding, and the direction of sliding is S-SE, the tilt of the layer has the same direction with topography, is SE-oriented and mostly bigger than  $5^\circ$ . It was understood that the deformations in the landslide mass were occurred from the geological unit, the layer or topography slope and precipitation and the landslide activity can continue in the study area. Thus, it has proven that precipitation and deformations within the layer are effective in triggering the landslide by the geodetic (IDH) observations, and it is understood that they were compatible with the geophysical results. Therefore, the study area contains the risk and the natural hazards, and these threatens the settlement area and the buldings and other constructions there.

### 1 Introduction

Today, large landslides occurring in Turkey have reached a considerable amount. It is known that a large landslide occurs in about every 5-10 years in Turkey (Över, 2015). These landslides usually occur in the forms of mud flow or mass movement. Three of the most effective of these landslides occurred in Koyulhisar (Sivas) in 19 August 1998, 20 July 2000 and 17 March 2005. Koyulhisar landslide area is one of the important large landslide areas in the country and occurs in the form of debris or mud flow (Fig. 1 and 8). In addition, Koyulhisar is an active landslide area, the activity of which has increased for the past 17 years. Koyulhisar landslide area, the subject of this article, is one of the largest landslide areas that significantly lead to serious loss of lives and property as in throughout Turkey. The large and small landslides in Koyulhisar landslide area have mostly occurred due to natural causes until today. Artificial causes mainly constitute the landslides caused by human interventions (blasting, drilling, improper planting, loading, loss of vegetation cover, etc.). The last large landslide occurred with the flow of mud in the north of Koyulhisar landslide area in March 2005. Duman et al. (2005) determined that this landslide was in the excessively fast (6 m/sec) class. Demirel vd. (2016), for the landslide in 2000 year revealed an average of 2.5-7.4 mm/year slip rate. Researchers have stated that these landslides usually have a mechanism involving a circular rotation, this old landslide mass maintains its activity and partial landslides occur on the groundmass (Sendir and Yılmaz, 2001; Duman et al., 2005). Therefore, Koyulhisar district center is on an old landslide that occurred in the form of circular rotation. The front of this landslide mass is open, it is always active, activity is not massive and usually in the form of local landslides occurring on the groundmass (Sendir and Yılmaz, 2001).



42 As it is known, landslides, as well as natural processes, may also occur with human-induced interventions  
43 (during blasting and excavation operations in many studies for roads, tunnels, and mines) performed on or near  
44 the landslide area (Lazzari, 2006). Therefore, it is important to investigate the reasons that affect the formation  
45 mechanisms and the formation of landslides. Different engineering (geology, geophysics, geodesic, etc.)  
46 disciplines have great role and importance especially in decreasing the negative effects. In this context,  
47 Koyulhisar landslide area was examined in a wide area with detailed GNSS (Global Navigation Satellite System)  
48 methods and the studies of other disciplines (Sendir and Yılmaz, 2002; Tatar et al., 2007; Hatiboğlu, 2009;  
49 Hastaoğlu and Şanlı, 2011; Yılmaz, 2009; Hastaoğlu, 2013; Türk, 2013; Topal and Hatiboğlu, 2015; Hastaoğlu,  
50 2015; Hastaoğlu, 2016). The annual sliding velocity, sliding direction, displacement amounts and natural disaster  
51 risk of the landslide have been identified by these studies. In these studies, it has been determined that the  
52 displacement amounts of the landslide velocity vary between 1-8.6 cm/year by topography and geological  
53 bedding and that the landslide direction is usually S-SE oriented. In terms of geology, some researchers have  
54 carried out geological studies on many issues such as geological, tectonic, geotechnical, geochemical and  
55 geomorphological studies at the local and regional scale in which the features of the faults, water, hot water, soil  
56 and rock on the NAFZ (North Anatolian Fault Zone) and in the region were investigated (Toprak, 1989; Uysal,  
57 1995; Sendir and Yılmaz, 2001; Sendir and Yılmaz, 2002; Yılmaz et al., 2005; Gökçeoğlu et al., 2005b; Duman  
58 et al., 2005; Ulusay et al., 2007; Hatiboğlu, 2009; Yılmaz, 2009; Demirel et al., 2016; Demir, 2018). The results  
59 of all these studies have been associated with geophysical results at the interpretation stage in this article.  
60 However, the geophysical studies, the subject of this article, were carried out for a limited area and have the  
61 distinction of being the first geophysical studies.

62 In the geophysical study, the hazards that would be caused by the landslide geometry of the last section in  
63 the close south of Koyulhisar landslide area and would affect the settlement area were investigated (Fig. 2 and  
64 8). The geophysical study was also carried out in this area which is the most active area of the landslide site  
65 because Hatipoğlu (2009) identified a movement of about 8.6 cm/year in this area. The SRT (Seismic Refraction  
66 Tomography) method determining the seismic P-wave velocities ( $V_p$ ) for seismic applications and the GPR  
67 (Ground Penetrating Radar) method for electromagnetic (EM) applications were used in the geophysical data  
68 collection in the area. In particular, seismic tomography (SRT, MASW) and ground penetrating radar (GPR)  
69 applications are the most commonly preferred methods in landslide studies. The structural geometry of the  
70 landslide area was determined by different parameters by assessing the collected geophysical data with  
71 appropriate software. These are the seismic  $V_p$  velocities, thickness, tilt and tilt direction of the layers. Thus,  
72 other features such as the sliding surface depth of the landslide, landslide type, advancement direction and the  
73 risk situation were also revealed, and geophysical and other study results were shown to be compatible with each  
74 other. The studies carried out by McCann and Forster (1990), Demirağ (1991), Hack (2000), Perrone et al.  
75 (2004), Göktürkler et al. (2008) are important in this regard. In addition, Bichler et al. (2004) carried out multi-  
76 methodical geophysical studies containing electrical resistivity, GPR and seismic methods in the landslide  
77 studies. Otto and Sass (2006) and Ristic et al. (2012) also carried out similar studies on landslide investigation.  
78 In these studies, the sliding surface of the landslides and the flow direction properties of the landslide material  
79 were generally determined by 2D (two-dimension) and 3D (three-dimension) geophysical sections.

80 It has been observed that the use of the SRT and GPR methods in landslide studies has increased  
81 significantly especially in recent years (Ristić et al., 2012; Timothy et al., 2013; Lissak et al., 2015; Hu and



82 Shan, 2016; Popescu et al., 2016; Su et al., 2016). The parameters which define the landslide such as landslide  
83 geometries and bedrock depth (sliding surface depth) have been determined in these studies. Regarding the GPR  
84 method, significant studies have been carried out by Davis and Annan (1989) on revealing the soil stratigraphy,  
85 by Aldaş et al. (2003), Slater and Niemi (2003) and Green et al. (2003) on the mapping of faults, fractures and  
86 cracks and by Benson (1995), Harari (1996), Bano et al. (2000) and Bubeck et al. (2015) on the determination of  
87 groundwater levels. However, the accurate determination of the landslide type is also very important as well as  
88 landslide elements. Joint studies with geophysics and other disciplines are commonly carried out in determining  
89 the landslide type and for different contributions. In addition to these, the seismological history, morphological  
90 and topographical features and meteorological data of the study area are always taken into account in the  
91 landslide analysis. They are largely used in such studies especially for their contribution to interpretation. In this  
92 article, the information obtained from all these data was used in order to make contributions to the geophysical  
93 results. For, landslides may develop under various geological, morphological, topographical and physical  
94 reasons. Thus, through multi-discipline studies, the landslide type can be determined most accurately by  
95 determining different sliding behaviors (such as the velocity and direction of the landslide, annual amount of  
96 displacement) varying from region to region. The landslides, which generally occur in the form of sliding, may  
97 occur with the movements of falling, sliding and flowing or with the combination of a few of these. Therefore,  
98 accurate determination of the landslide type/kind and the selection of the methods used in the study is very  
99 important. It may be possible to perform an accurate landslide analysis only if these requirements are met.

## 100 **2 Geology**

101 The study area is about 180 km away from Sivas city center and is in the west of Koyulhisar district center which  
102 is located in the north of the NAFZ (Fig. 1 and 8). The rocks in the region usually have fractures and  
103 discontinuities and are crushed because of the NAFZ which is tectonically active in south of the study area  
104 (Tatar et al., 2005). There are also many old and new landslides in the study area depending on the high tilted  
105 topography. For these reasons, the directions of movement of the landslides generally threaten the settlement  
106 areas (Sendir and Yılmaz, 2001). The geological investigation of Koyulhisar has been carried out regionally or  
107 locally by various researchers (Terlemez and Yılmaz, 1980; Toprak, 1989; Uysal, 1995; Sendir and Yılmaz,  
108 2002; Duman et al., 2005; Hatiboğlu, 2009). According to these studies, the Plio-Quaternary aged Koyulhisar  
109 Formation is the youngest unit in the region. It was stated that the youngest unit consisted of the talus (slope or  
110 deposit) and fluvial conglomerates and was seen along the strike-slip faults (Toprak, 1989).

111 Toprak (1989) divided the NAFZ which is represented by a right lateral strike-slip fault zone into five  
112 fault sets including the North Anatolian Main Fault, Koyulhisar fault sets, Kelkit fault set, Şihlar fault set and  
113 Kuruçay fault set. But, the Şihlar fault sets affect Koyulhisar district center at the nearest (Fig. 1). Toprak (1989)  
114 stated that Koyulhisar section of the NAFZ is still active and a right lateral strike-slip fault zone due to the  
115 morphotectonic structures and seismic activities in the region (Fig. 1). As it is seen in Fig. 1, the faults closely  
116 concerning Koyulhisar are the NAFZ, which is the main fault extending in the northwest-southeast direction and  
117 approximately 2-2.5 km away, in the south, and the Çamlıyaka Fault, which is approximately north-south-  
118 oriented, in the west. This fault which is the closest one to the study area extends perpendicular to the NAFZ  
119 in the south. It was also reported by Tatar et al. (2007) that large and old landslide masses in Koyulhisar landslide  
120 area have lower Miocene-aged clay and gypsum levels, Eocene-aged clayey levels and Plio-Quaternary aged  
121 sediments.



122 The large and small landslides in Koyulhisar landslide area have mostly occurred due to natural causes  
123 until today. The landslides in and near the study area were triggered by old cracks, displacements, and  
124 seismotectonic effects over time because they are on the NAFZ (North Anatolian Fault Zone) which is the  
125 largest and most active fault zone in Turkey. The geology, morphology and flora features of the study area and  
126 its surrounding have also been the other factors that triggered the landslide. Therefore, the studies carried out in  
127 the region have shown that active faults triggered the landslides due to the geological and lithologic features of  
128 the region.

### 129 3 Methods

#### 130 3.1 Geophysical surveys

131 The SRT (Seismic Refraction Tomography) and GPR (Ground Penetrating Radar) methods which are applied in  
132 tomography format were used in the geophysical study. Before applying the SRT and GPR methods in the field,  
133 the study area was named as A-C and the geophysical measurements were collected separately in these areas  
134 (Fig. 2). Then, the geophysical profiles were processed to the satellite map according to the coordinates along  
135 with the topographical elevation curves and GNSS measurement locations for the ease of interpretation (Fig. 2a).  
136 Geophysical measurements were taken as both NE-SW and NW-SE oriented due to the geologic bedding and  
137 topographic features (Fig. 2b-c). However, SRT12-GPR12 profiles were selected as about E-W oriented due to  
138 rugged topography in area C. The profile lengths usually range from 40 to 60 m according to the method applied.  
139 10 SRT measurements were taken in all areas in the seismic study for geophysical measurements. 10 profile  
140 GPR measurements were taken in areas A and C in the electromagnetic study. The profile shooting technique in  
141 the field, hammer and iron plate of 8 kg weight as the source and 12 P geophones of 14 Hz and Geometrics  
142 branded seismic device as the receiver were used while collecting the SRT data. In all profiles, the geophone  
143 interval was 5 m, offset distance was 2.5 m, sampling interval was 256 ms and the record length was 512 ms.  
144 The geophones were respectively fixed on the ground within the selected geophone range and their connections  
145 with the seismic device were made. Then, seismic measurements were recorded by starting from the offset  
146 distance of 2.5 m, reducing to sledgehammer plate and making at least 5 shots between each geophone,  
147 respectively.

148 There are 2 close NE-SW (SRT2, SRT4) oriented seismic SRT profiles and 2 NW-SE oriented seismic  
149 SRT profiles in the area defined by A in Fig. 2b. There a total of four GPR profiles on these seismic profiles  
150 including NE-SW oriented (GPR2 and GPR4) and NW-SE oriented (GPR3 and GPR5). In area C, there are close  
151 E-W oriented SRT10 and SRT11 profiles in the west of the area and GPR10 and GPR11 profiles on these  
152 profiles, and SRT9 and SRT14 profiles in the close NE-SW direction in the same area and GPR9 and GPR14  
153 profiles located over them (Fig. 2c). There are E-W oriented SRT12 and close NE-SW oriented SRT13 and  
154 GPR12 and GPR13 profiles located over them in the east direction of the area.

155 In addition, the landslide cracks on the surface, displacement traces, and structural damages in the study  
156 area and its immediate surroundings can be monitored clearly by field observations (Fig. 3). Some landslides in  
157 the study area and a portion of the landslide crack traces and the damaging effects of still active or old landslides  
158 on buildings can easily be observed in Fig. 3 All damaged structures across the region cannot be used. Therefore,  
159 new landslide cracks will emerge over time both on the ground and the existing structures in the region which  
160 active in terms of landslide and seismicity, and the formation of new landslides will continue in the area.

#### 161 3.2 Results, analysis and discussion



162 In the evaluation of the SRT data collected in the field, SeisImager program was used for displaying, processing  
163 and evaluation of the seismic refraction waves. The marking of the first arrivals of the SRT data was performed  
164 using Pickwin, and the evaluation of the first arrival data was performed using Plotrefa module. The GPR data  
165 collected on the SRT profiles only in the areas A and C were collected by Ramac2 device using a closed antenna  
166 of 250 MHz. The GPR data were processed in Reflexw program. The time-depth sections which were ready for  
167 interpretation were obtained by increasing the signal/noise ratios of the signals in the data processing. The  
168 geophysical sections were prepared by also making a topographic correction in the inversion operation due to the  
169 variability of the topography. Thus, the collected geophysical data were converted into 2D (two-dimension)  
170 height-distance and depth-distance sections by being assessed in the appropriate software. Geophysical  
171 interpretations were made according to these sections and compared with the results of the other studies.  
172 Accordingly, 2D (two-dimension) seismic cross-sections giving seismic  $V_p$ -depth information are presented in  
173 Fig. 4 and 5. In the seismic data evaluation, the coincidence was provided with RMS (Root Mean Square) errors  
174 ranging between 3.4-4.5% in 2D (two-dimension) inversion operation. According to 2D (two-dimension)  
175 seismic cross-sections, two or three layers were identified at about 20 m depth. It was understood that the tilts of  
176 these layers were southeast oriented, and their tilt was greater than 50. According to seismic velocities ( $V_p$ )  
177 calculated, three layers with the layer velocities of 0.30, 1.00 and 2.00 km/s on average were defined from top to  
178 bottom.  $V_p$  values of these layers increase towards the deep. Layer thicknesses range between 3 m and 6.5 m on  
179 average from top to bottom due to topographical differences. It was understood that the depth of the sliding  
180 surface varied between about 7-10 m, and these depths were the upper bound of the third layer. The units are  
181 loose up to this depth according to geological drilling logs (Hatipoğlu, 2009; Hastaoğlu, 2015). This area was  
182 considered to have a risk of dislocation due to these loose units, rainfall and tilt conditions. Therefore, the layers  
183 with an average of  $V_{p1}=0.3$  km/s and  $V_{p2}=1.00$  km/s over these depths were defined as the layers with the risk of  
184 dislocation. The layer with a seismic velocity of greater than  $V_{p3}>2.00$  km/s at the lowermost was understood to  
185 be the basement layer. On the other hand, the investigation depth was further calculated from the SRT sections  
186 compared to the GPR sections due to the differences of geophysical methods in the application. Because GPR  
187 sections could be obtained as high resolution for about the first 10 m depth after inversion processing of the GPR  
188 data (Fig. 6 and 7). Therefore, it could be said that the GPR and SRT sections are compatible for the first 10 m  
189 depth. Besides, the profile lengths of the GPR3 and GPR5 sections in Fig. 7 were evaluated as about 25-35 m.

190 According to the GPR sections in Fig. 6 and 7, there is a layer with a varying thickness of about 3 mm at  
191 the uppermost. It is seen that the second layer under this layer proceeds until about 7-10 m depth. These layers  
192 are weak, loose and reworked layers with refractions that lost their thickness with low seismic velocity.  
193 However, three layers were identified in seismic sections, and their seismic velocity was observed to increase  
194 towards the depth ( $0.30 < 1.00 < 2.00 < \dots$  km/s). Accordingly, the fact that the problems seen in the first two layers  
195 decreased and ended towards deeper layers ( $>7-10$  m) is understood from the increase in seismic velocities  
196 ( $>2.00$  km/s). Therefore, it was understood from the geophysical and geological data obtained for the landslide  
197 basement and the layer over it that new landslides may occur over time in the study area due to the tilt and  
198 abrasion and transports during precipitation.

199 The electromagnetic wave velocity in the GPR sections is  $V=0.1$  m/ns. This value is generally observed in  
200 dry or wet soil, dry or wet clay and sandy environments (Wilchek, 2000; Cardomina, 2002). The high-frequency  
201 electromagnetic waves can reach deeper in the environments with low conductivity like sand. However, the



202 conductive units such as clay and shale decrease the penetration depth of the signal transmitted and lead to  
203 absorption (Annan et al., 1988; Davis and Annan, 1989). Hatiboğlu (2009) and Hastaoğlu et al. (2015) generally  
204 observed two geological units in the wells in the study area. They observed that the upper unit was silty sandy  
205 clay and sand interbedded silty clay in some places up to about 10 m, and advanced as sand interbedded silty  
206 clay and sand interbedded clay in some places towards deeper than 10 m. Therefore, it was understood that this  
207 velocity value was compatible with the units and electromagnetic waves led to rapid absorption due to the layers  
208 with clay content. Furthermore, sliding surfaces, landslide furrows, scarps, cracks was observed in the GPR  
209 cross-sections, in A and C area (Fig. 6 and 7). In other words, the geological unit, the layer or topography slope  
210 and precipitation cause deformations in the loose upper unit. Therefore, these structures may develop or occur in  
211 the landslide mass, as shown in Fig. 6 and 7.

### 212 3.3 Seismological and meteorological data and results

213 The study area is located in an active area in terms of seismicity. The seismological history, the magnitude (M)  
214 of which is greater than 2.5, of the examined area and its surrounding between 1900-2015 were investigated for  
215 this article (Fig. 8). The map in Fig. 8 was prepared with the seismological data between 1900-2015 (UDİM,  
216 2016). Particular attention was paid to the earthquakes before 2005 in the seismological interpretation. This is  
217 because the largest and most recent landslide occurred in the area in 2005 and it was aimed to investigate its  
218 relationship with displacements and previous landslides. The type of magnitude which is calculated from  
219 seismological data is usually the local magnitude. The depths (d) of these earthquakes with higher  $M > 2.5$  vary  
220 between approximately 5 and 80 km (Fig. 8). According to the seismic data of the years examined, Koyulhisar  
221 and its surroundings have always been active seismically. It was observed that this frequency of earthquakes  
222 usually occurred on the NAFZ in the south of the study area. Additionally, it has been analyzed the seismic  
223 activity of the region at least for the last 112 (1904-2016) years by Demir (2018). In this study, he express that  
224 the most notable is probably the relationships between the magnitude of the earthquake to the number of  
225 landslides and the area affected by the landslides and between the magnitude and the maximum distance of  
226 landslide observations from the epicenter in different geological, topographical, and climatic conditions (Demir,  
227 2018).

228 Large earthquakes affecting Koyulhisar district also occurred in the region. These largest earthquakes are  
229 in the south of the NAFZ or Suşehri district and a total of three large earthquakes with  $M \geq 5.6$  occurred there  
230 (Över, 2015). Among these, 1992 earthquake is closest to the study area with the least depth but the second  
231 largest earthquake (Fig. 8). This earthquake is an earthquake with 6.1 magnitude that occurred 10 km below the  
232 ground. The large earthquakes in the south of Suşehri district which is just 13 km away from the study area  
233 occurred in 1909 and 1939. 1909 earthquake occurred 60 km below the ground and is the largest and deepest  
234 earthquake with a magnitude of 6.3. 1939 earthquake is also deep and the third largest earthquake that occurred  
235 50 km below the ground with a magnitude of 5.6 (Över, 2015). In addition, when Fig. 8 is analyzed, it is seen  
236 that the magnitudes of the other earthquakes in the north of the NAFZ and the upper elevations of the landslide  
237 generally vary between 2.5-4. Similarly, it is seen that the other earthquakes in the south of the landslide area are  
238 the earthquakes with a magnitude of greater than 3.6. All these earthquakes may have triggered the landslide  
239 mass from time to time in places where sliding surfaces, layers, and topography in the landslide area are more  
240 inclined than 5-10 degrees (according to the geophysical cross-sections in this article, when it is considered that



241 there are loose units and deformations on the sliding surfaces). In particular, they further affected the landslide  
242 mass along with the rain and caused large amounts of displacement in the landslide area.

243 The data regarding the rainfalls with the effects of triggering the landslides are presented in Table 1 and  
244 Fig. 9 (MGM, 2016). With these data, the rainfall status of the study area and its surrounding was examined by  
245 months as average annual rainfalls and the annual areal amount of rainfall. According to the data obtained  
246 between 1950-2015 in Table 1, the rainy periods are generally between October-November-December and  
247 January-February-March-April. The highest total daily amount of rainfall in the rainiest years was observed as  
248 snowfall in 1950 (110 cm) and as rain in 1991 (55 kg/m<sup>2</sup>).

249 According to Fig. 9, the annual normal average rainfall value calculated for the years between 1981-2010  
250 was calculated as over 483.4 mm. However, 1987-1988 and 1997-1998 were the rainiest years. It is seen that the  
251 annual areal amount of rainfall exceeded the normal values and was higher than 550 mm in these rainy years that  
252 took place in every 10 years. Similarly, it is also seen that there were high rainfalls for 3-4 years after the years  
253 of 1985-1995-2005 with an interval of 10 years. Therefore, annual areal rainfalls were observed to be more  
254 before some large landslides like the landslide in 1998. When geological features of the region are taken into  
255 account, it is remarkable that the landslide in 1998 and 2000 occurred in the summer months after the winter  
256 with a heavy fall of snow. However, the landslide in 2005 occurred during the rainy season. Therefore, rainfalls  
257 have always been considered as a factor triggering these landslides in many studies and articles (Tatar et al.,  
258 2007; Hastaoğlu et al., 2015). Similarly, the authors of this article have always considered rainfalls as a  
259 triggering factor in the formation of Koyulhisar landslides. As it is seen, the various studies and the results of  
260 this article have proved that Koyulhisar landslides are generally caused by the known reasons that trigger the  
261 landslide. Because the seismic activity, the meteorological data and the other conditions mentioned in the  
262 landslide area have shown that the landslides could be triggered there.

### 263 3.4 Geodetic surveys and results

264 Hastaoğlu et al. (2015) have carried out multi-disciplinary studies and GNSS studies for many years (about 6  
265 years) to determine the deformation and annual sliding amounts especially after the landslides in 1998-2000-  
266 2005. It was determined that the tension cracks that occurred in the landslides in 1998 and 2000 in the region  
267 were filled with the waters consisting of melting snow and rain waters which are the most important component  
268 of the hydrological cycle, lakes were formed in the buttress of each sliding mass, and the changes in the  
269 groundwater level were the main causes of deformation (Sendir and Yılmaz, 2001; Topal and Hatiboğlu, 2015;  
270 Hastaoğlu et al., 2015). The seismological and meteorological data, which were updated by the geodetic (GNSS  
271 (DH), geological (IDH (Inclinometer Drilling Holes)) and meteorological data collected in the local study of  
272 Hastaoğlu et al. (2015), were reorganized and evaluated. Fig. 2, 9, 10 and Table 1 which were reprepared for the  
273 study which is the subject of this article were associated with the results of GNSS studies (Fig. 10). Then, they  
274 were compared with geophysical results in interpretation.

275 The monthly and annual meteorological data should certainly be evaluated particularly within the scope of  
276 monitoring activities because the area which is the subject of the study is a landslide area. Hastaoğlu et al. (2015)  
277 performed monitoring in IDH wells in the area in 2013-2014 (Fig. 10). If Fig. 2 is examined, there are seven  
278 IDH point in the nearest of the geophysical profiles. The graphics in Fig. 10 were prepared from the combined  
279 data (unpublished data in the project) and the temperature (°C), precipitation (m<sup>3</sup>) and soil moisture content (cm)  
280 were compared in these graphics. Accordingly, the temperature and precipitation were observed to be inversely



281 proportional during the summer months called as a dry period. It is seen that the soil moisture is changeable  
282 apart from the rainy period and has very high water content during the rainy periods. On the other hand, it was  
283 understood that the precipitation increased by the decrease in temperatures. It is also seen that the total annual  
284 amount of rainfall increased about 2-fold in 2014 compared to 2013 (Fig. 9 and 10). According to all results,  
285 rainfalls are considered to be effective in triggering of the landslide because the ground of this landslide area,  
286 which is filled with loose units and old cracks, is supersaturated with water due to the rainfalls.

287 Besides, Hastaoğlu et al. (2015) determined that the groundwater level gets close to the surface for 4-6 m  
288 on average at the end of the rainy period, to 10 m at the end of the rainy period and decreases up to 25 m in some  
289 wells in the area where geophysical study area is also located, and the groundwater flow direction is SW. When  
290 this information was associated with topography and in line with the field observations, it was understood that  
291 the topography was inclined from the north of the study area towards south, the incline of slope decreased from  
292 925 m to 840 m, there was an elevation difference of 85 m, and the amount of slope in the topography increased  
293 from south to north ( $>5^{\circ}$ - $10^{\circ}$ ) (Fig. 2a). Therefore, it was seen that the geological bedding was compatible with  
294 the topographical sloping and the groundwater was compatible with the direction of flow. Hatiboğlu (2009) and  
295 Hastaoğlu et al. (2015) observed that the geological units advanced as silty sandy clay from top to bottom and  
296 partly sand interbedded silty clay under the topsoil and as sand interbedded silty clay and sand interbedded clay  
297 in some places towards deeper than about 10 m in IDH wells in the geophysics study area. Hastaoğlu et al.  
298 (2015) estimated with the GPS measurements that the amounts of displacement varied between 1-8.6 cm/year.  
299 The geophysical data were collected in the areas where the amount of displacement varied about 8.6 cm/year.  
300 The landslide direction was determined to be in the S-SW and SE direction across Koyulhisar (Hastaoğlu et al.,  
301 2015). It was understood that these directions were compatible with the geophysical sections which were  
302 prepared later and that the rainfalls are among the reasons that trigger the landslide.

#### 303 **4 Conclusions**

304 This study is the first geophysical study carried out in Koyulhisar landslide area. The information provided from  
305 many studies (geodetic, geologic, morphologic, seismological, topographic and meteorological) carried out  
306 across the region was compared with the geophysical results (SRT and GPR) and found to be compatible. The  
307 bedding status of the landslide area, seismic P-wave velocity ( $V_p$ ) of the layers, the tilt, tilt direction of the  
308 layers, depth of the sliding surface and sliding direction and the landslide type could be determined from the  
309 geophysical sections. Accordingly, the study area was identified by the layers with the average seismic velocities  
310 of  $0.30 < 1.00 < 2.00 < \dots$  km/s (or 300, 1000 and 2000 m/sec). The seismic velocity of the landslide basement  
311 was found to be higher than 2000 m/sec. According to the geophysical cross-sections, it was understood that the  
312 depth of the sliding surface varied between 7-10 m due to the topographical differences. These depths are the  
313 depths with low seismic velocities (the average  $V_p$ ,  $<0.30$  and  $<1.00$  km/s) and defined as loose units which were  
314 also observed in geological drilling logs. It is understood that sliding surfaces, landslide furrows, collapsed  
315 zones, scarps, cracks are observed in the GPR sections. Furthermore, it was understood that the layer tilt was  
316 generally more than  $5^{\circ}$  in all geophysical sections and compatible with the geology and the flow direction of the  
317 groundwater. It was understood that the landslide type in the area was planar sliding and the direction of sliding  
318 was SE.

319 The geophysical and geodetic study results were found to be compatible because it is known that the  
320 landslide direction across Koyulhisar is in S-SW and SE. Consequently, the fact that the depth of the sliding



321 surface over the units is loose, low seismic velocities of the upper layers and the excessive tilt prove that there is  
 322 a new risk of landslide in the area. The other factors that trigger the landslide were found to be associated  
 323 especially with the fact that the area is seismically active, receives heavy rain and has a poor vegetation cover.  
 324 Furthermore, it was understood that there were deformations in the landslide mass and, observed the sliding  
 325 surfaces, landslide furrows, collapsed zones, scarps and cracks structures. It was understood that these structures  
 326 were occurred from the geological unit, the layer or topography slope and precipitation. On the other hand, it was  
 327 understood that studies such as blasting and excavation performed by human intervention can trigger the  
 328 landslides and hence the landslide area is a potential area which is open to natural/artificial hazards. As a result,  
 329 according to all the results, there is still a high landslide hazard in the study area and its surrounding, and this  
 330 hazard will be also in the future. As a result, the identified risks and natural hazards are also threatened the  
 331 settlement area and the buildings and other constructions (e.g. roads, walls, parks et al.) there.

332 **Acknowledgments:** This study was supported by Cumhuriyet University Scientific Research Projects  
 333 Commission as CÜBAP Project numbered M-464. We would like to thank Project Coordinator Assoc. Dr.  
 334 Kemal Özgür Hastaoğlu and his research team, who allowed us to benefit from the results of TÜBİTAK  
 335 supported project numbered 111Y111, for their contributions. We would like to thank Dr. Çağrı Çaylak for his  
 336 contributions during the geophysical field measurements, Assoc. Dr. Fatih Poyraz for his contributions during  
 337 the process of geodetic field measurements and Assoc. Dr. Tark Türk. We would like to thank Geological  
 338 Engineer Mehmet Demirel for his contributions to the Fig. 2.

### 339 References

- 340 Adlaş, G. U., Kadioğlu, S., Ulugergerli, E. U.: The effects of concealed discontinuities in blast design Pattern, 4th Int.  
 341 Scientific and Technical Conference of Young Scientists and Specialists, St. Petersburg-RUSSIA, 6-7, 2003.
- 342 Bano, M., Marquis, G., Niviere, B., Maurin, J. C., Cushing, M.: Investigating alluvial and tectonic features with ground  
 343 penetrating radar and analyzing diffractions patterns, *J. Appl. Geophys.*, 43, 3-41, 2000.
- 344 Benson, A. K.: Applications of ground penetrating radar in assessing some geological hazards: Examples of groundwater  
 345 contaminants, faults, cavities, *J. Appl. Geophys.*, 33, 177-193, [https://doi.org/10.1016/0926-9851\(95\)90040-3](https://doi.org/10.1016/0926-9851(95)90040-3), 1995.
- 346 Bichler, A., Bobrowsky, P., Best, M., Douma, M., Hunter, J., Calvert, T., Burns, R.: Three-dimensional mapping of a  
 347 landslide using a multi-geophysical approach: the Quesnel Forks landslide, *Landslides*, 1, 29-40, DOI 10.1007/s10346-  
 348 003-0008-7, 2004.
- 349 Bubeck, A., Wilkinson, M., Roberts, G. P., Cowie, P. A., McCaffrey, K. J. W., Phillips, R., Sammonds, P.: The tectonic  
 350 geomorphology of bedrock scarps on active normal faults in the Italian Apennines mapped using combined ground  
 351 penetrating radar and terrestrial laser scanning, *Geomorphology*, 237, 38-51, DOI:10.1016/j.geomorph.2014.03.011, 2015.
- 352 Cardimona, S.: Subsurface investigation using ground penetrating radar, Presented at the 2nd International Conference on the  
 353 Application of Geophysics and NDT Methodologies Transportation Facilities and Infrastructure, Los Angeles, California,  
 354 2002.
- 355 Davis, J. L., Annan, A. P.: Ground-penetrating radar for high resolution mapping of soil and rock stratigraphy, *Geophys.*  
 356 *Prosp.*, 37, 531-551, DOI: 10.1111/j.1365-2478.1989.tb02221.x, 1989.
- 357 Demir, G.: Landslide susceptibility mapping by using statistical analysis in the North Anatolian Fault Zone (NAFZ) on the  
 358 northern part of Suşehri Town, Turkey, *Nat. Hazards*, 92, 133-154, <https://doi.org/10.1007/s11069-018-3195-1>, 2018.
- 359 Demirağ, O.: Jeofizik yöntemlerle heyelan araştırmaları, TMMOB-JFMO (The Chamber of Geophysical Engineers of  
 360 Turkish) publications, *Jeofizik*, 5(1); 43-50, Ankara, Turkey, 1991 (in Turkish).
- 361 Demirel, M., Tatar, O., Koçbulut, F.: Kinematics of the faults around the Koyulhisar (Sivas) region on the North Anatolian  
 362 Fault Zone, *Geol. Bull., Turkey*, 59(3), 357-370, 2016 (in Turkish).
- 363 Duman, T. Y., Nefeslioğlu, H., Gökçeoğlu, C., Sönmez, H.: 17/03/2005 Kuzulu (Sivas-Koyulhisar) heyelanı, Maden Tetkik  
 364 ve Arama Genel Müdürlüğü Jeoloji Etütleri Dairesi, Hacettepe Üniversitesi, 2005.
- 365 Gren, A., Gross, R., Holliger, K., Horstmeyer, H., Baldwin, J.: Results of 3D georadar surveying and trenching the San  
 366 Andreas fault near its northern landward limit, *Tectonophysics*, 368, 7-23, doi:10.1016/S0040-1951(03)00147-1, 2003.
- 367 Gökçeoğlu, C., Nefeslioğlu, H. A., Sönmez, H., Duman, T., Can, T.: The 17 March 2005 Kuzulu landslide (Sivas, Turkey)  
 368 and landslide-susceptibility map of its near vicinity, *Eng. Geol.*, 81 (1), 65-83, DOI:10.1007/s00254-006-0322-1, 2005b.
- 369 Göktürkler, G., Baklaya, Ç., Erhan, Z.: Geophysical investigation of landslide: The Altındağ landslide site, Izmir (western  
 370 Turkey), *J. Appl. Geophys.*, 65, 84-96, <https://doi.org/10.1016/j.jappgeo.2008.05.008>, 2008.
- 371 Hack, R.: Geophysics for slope stability, *Surv. Geophys.*, 21, 423-338, 2000.
- 372 Harari, Z.: Ground penetrating radar (GPR) for imaging stratigraphic features and groundwater in sand dunes, *J. Appl.*  
 373 *Geophys.*, 36, 43-52, [https://doi.org/10.1016/S0926-9851\(96\)00031-6](https://doi.org/10.1016/S0926-9851(96)00031-6), 1996.

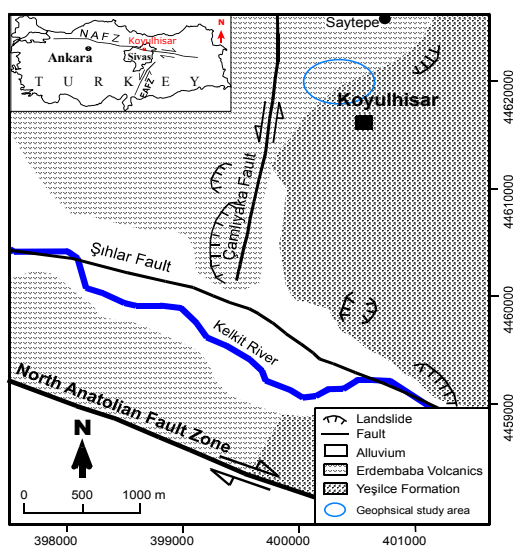


- 374 Hastaoğlu, K. O.: Investigation of the groundwater effect on slow-motion landslides by using dynamic Kalman filtering  
375 method with GPS: Koyulhisar town center, Turkish J. Earth Sci., 1033-1046. DOI: 10.3906/yer-1210-10. 2013.
- 376 Hastaoğlu, K. O., Şanlı, D. U.: Monitoring Koyulhisar landslide using rapid static GPS: a strategy to remove biases from  
377 vertical velocities, Nat. Hazards, 58, 1275-1294, DOI:10.1007/s11069-011-9728-5, 2011.
- 378 Hastaoğlu, K. O.: Comparing the results of PSInSAR and GNSS on slow motion landslides, Koyulhisar, Turkey, Geomatics,  
379 Nat. Hazards and Risk, 7, 2, 786-803, DOI: 10.1080/19475705.2014.978822, 2016.
- 380 Hatiboğlu, O.: Investigation Of Koyulhisar (Sivas) Settlement Area In Terms of Slope Instability, Middle East Technical  
381 University, MS Thesis, Ankara, Turkey, 2009.
- 382 Hu Z., Shan W.: Landslide investigations in the northwest section of the lesser Khingan range in China using combined HDR  
383 and GPR methods, Bull. Eng.. Geol. Environ., 75, 591-603, DOI 10.1007/s10064-015-0805-y, 2016.
- 384 Lazzari, M., Gerdali, E., Lapenna, V., Loperte, A.: Natural hazards vs human impact: an integrated methodological approach  
385 in geomorphological risk assessment on the Tursi historical site, Southern Italy, Landslides, 3, 275-287. DOI  
386 10.1007/s10346-006-0055-y, 2006.
- 387 Lissak, C., Maquaire, O., Malet J.P., Lavigne, F., Virmoux, C., Gomez, C., Davidson, R.: Ground-penetrating radar  
388 observations for estimating the vertical displacement of rotational landslides, Nat. Hazards Earth Syst. Sci., 15, 1399-  
389 1406, doi:10.5194/nhess-15-1399-2015, 2015.
- 390 McCann, D. M., Forster, A.: Reconnaissance geophysical methods in landslide investigations, Eng Geol 29(1):59-78,  
391 [https://doi.org/10.1016/0013-7952\(90\)90082-C](https://doi.org/10.1016/0013-7952(90)90082-C), 1990.
- 392 MGM: Meteoroloji Genel Müdürlüğü (Turkish State Meteorological Service), Ankara Meteoroloji Bölge Müdürlüğü'nün  
393 Hidrotermal Şube Müdürlüğü (Hydrothermal Directorate of Ankara Meteorology Regional Directorate).  
394 <https://www.mgm.gov.tr/> (accepted: 12.11.2008), 2016.
- 395 MTA: General Directorate of the Mineral Research and Exploration (MTA), (last access: 11.04.2018),  
396 <http://yerbilimleri.mta.gov.tr/anasayfa.aspx>, 2018.
- 397 Otto, J. C., Sass, O.: Comparing geophysical methods for talus slope investigations in the Turtmann valley (Swiss Alps),  
398 Geomorphology, 76, 257-272, doi:10.1016/j.geomorph.2005.11.008, 2006.
- 399 Över, D.: The Research of The landslide area ground of Koyulhisar district in Sivas with geophysical methods,  
400 Cumhuriyet University, MS Thesis, Sivas, Turkey, 2015.
- 401 Perrone A., Iannuzzi, A., Lapenna, V., Lorenzo, P., Piscitelli, S., Rizzo, E., Sdao, F.: High-resolution electrical imaging of  
402 the Varco d'Izzo earthflow (southern Italy), J. Appl. Geophys., 56, 17-29, DOI:10.1016/j.jappgeo.2004.03.004, 2004.
- 403 Popescu, M., Şerban, R. D., Urdea, P., Onaca, A.: Conventional geophysical surveys for landslide investigations: Two case  
404 studies from Romania, Carpathian J. Earth and Environ. Sci., 11(1), 281-292, 2016.
- 405 Ristić, A., Abolmasov, B., Govedarica, M., Petrovački, D.: Shallow-Landslide Spatial Structure Interpretation Using A  
406 Multi-Geophysical Approach, Acta Geotechnica Slovenica, 47-59, 2012.
- 407 Sendir, H., Yılmaz, I.: Koyulhisar Heyelanlarına Yapısal ve Jeomorfolojik Açından Bakış, Cumhuriyet Üniversitesi  
408 Mühendislik Fakültesi Dergisi, Seri A: Yer Bilimleri, 18 (1), 47-54, 2001 (in Turkish).
- 409 Sendir, H., Yılmaz, I.: Structural, geomorphological and geomechanical aspects of the Koyulhisar landslides in the North  
410 Anatolian Fault Zone (Sivas, Turkey), Environ. Geol., 42, 52-60, <https://doi.org/10.1007/s00254-002-0528-9>, 2002.
- 411 Slater, L., Niemi, T. M.: Ground penetrating radar investigation of active faults along the Dead Sea transform and  
412 implications for seismic hazards within the city of Aqaba, Jordan, Tectonophysics, 368, 33-50, 2003.
- 413 Su, L., Xu, X., Geng, X., Liang, S.: An integrated geophysical approach for investigating hydro-geological characteristics of  
414 a debris landslide in the Wenchuan earthquake area, Eng. Geol., <http://dx.doi.org/10.1016/j.enggeo.2016.11.020>, 2016.
- 415 Tatar, O., Gürsoy, H., Gökçeoğlu, C., Koçbulut, F., Duman, T. Y., Kök S., Süllü, H., Şenyurt, A., İleri, N.: 17 Mart 2005  
416 Sivas İli Koyulhisar İlçesi Sugözü Köyü Kuzulu Mahallesi Heyelanı 2. Değerlendirme Raporu,  
417 <http://www.koyulhisar.gov.tr/bulten3.doc..>, 2005 (in Turkish).
- 418 Tatar, O., Gürsoy, H., Altunel, E., Akyüz, S., Topal, T., Sezen, T. F., Koçbulut, F., Mesci, L., Kavak, K.Ş., Dikmen, Ü.,  
419 Türk, T., Poyraz, F., Hastaoğlu, K., Ayazlı, E., Gürsoy, Ö., Polat, A., Akın, M., Demir, G., Zabcı, C., Karabacak, V.,  
420 Çakır, Z.: Kuzey Anadolu Fay Zonu üzerinde Kelkit Vadisi boyunca yer alan yerleşim alanlarının doğal afet risk analizi,  
421 CBS tabanlı afet bilgi sistemi (KABİS) tasarımı: Proje tanıtımı ve ön bulgular. Aktif Tektonik Araştırma Grubu 11.  
422 Çalıştayı, TÜBİTAK-MAM Yer ve Deniz Bilimleri Enstitüsü Gebze-Kocaeli, Türkiye, 14-16, 2007 (in Turkish).
- 423 Terlemez, İ., Yılmaz A.: Ünye-Ordu-Koyulhisar-Reşadiye arasında kalan yöreinin stratigrafisi, TJK Bülteni, 21, 179-191, 1980  
424 (in Turkish).
- 425 Timothy R. H. Davies, Warburton J., Stuart A. Dunning, Alodie A. P. Bubeck: A large landslide event in a post-glacial  
426 landscape: rethinking glacial legacy, Earth Surface Processes and Landforms, 38(11), 1261-1268,  
427 <https://doi.org/10.1002/esp.3377>, 2013.
- 428 Topal, T., Hatiboğlu O.: Assessment of slope stability and monitoring of a landslide in the Koyulhisar settlement area (Sivas,  
429 Turkey), Environ. Earth Sci., 74(5), DOI 10.1007/s12665-015-4476-6, 2015.
- 430 Toprak, G. M. V.: Tectonic and stratigraphic characteristics of the Koyulhisar segment of the North Anatolian Fault Zone  
431 (Sivas-Turkey), METU (unpublished), PhD. Thesis, Ankara, Turkey, 121, 1989.
- 432 Türk, T.: Hava fotoğrafı ve optik uydu görüntüleri yardımıyla yatay yer değişimlerinin belirlenmesi, Havacılık ve Uzay  
433 Tekn. Derg., 6 (1), 71-79, 2013 (in Turkish).
- 434 UDİM: Ulusal Deprem İzleme Merkezi (National earthquake monitoring center), Boğaziçi University KOERI (Kandilli  
435 Observatory And Earthquake Research Institute), [www.koeri.boun.edu.tr/sismo/](http://www.koeri.boun.edu.tr/sismo/), (last access: 11.04.2018), İstanbul,  
436 Turkey, 2015.
- 437 Uysal, S.: Koyulhisar (Sivas) yöresinin jeolojisi, General Directorate of the Mineral Research and Exploration (MTA) Report  
438 number: 9838, 1995 (in Turkish).
- 439 Ulusay, R., Aydın, Ö., Kılıç, R.: Geotechnical assessment of the 2005 Kuzulu landslide (Turkey), Eng. Geol., 89(1-2), 112-  
440 128, 2007.



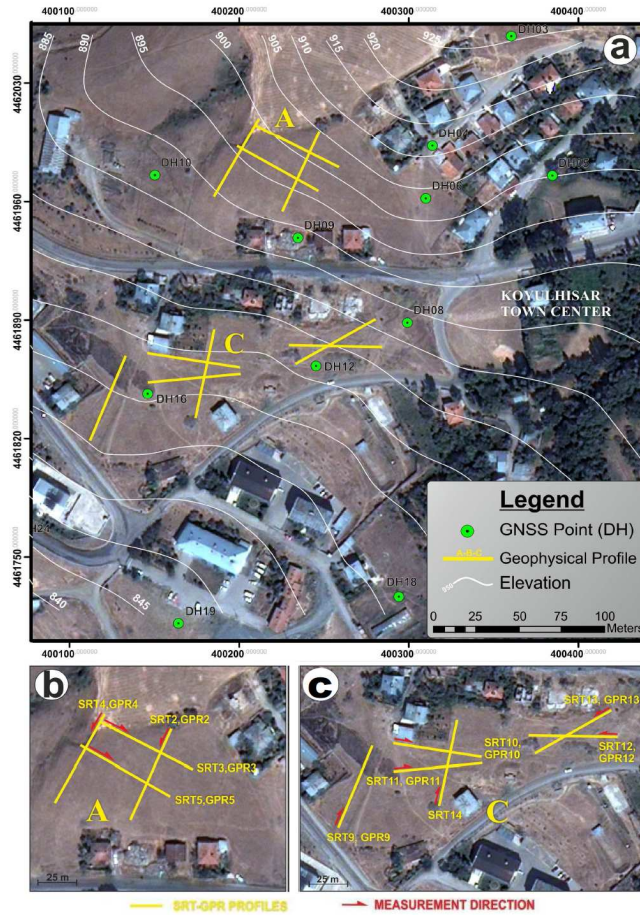
- 441 Wilchek, L.: Ground Penetrating Radar for Detection of Rock Structure, MS Thesis, Alberta University, Canada, 2000.  
442 Yılmaz, I.: A case study from Koyulhisar (Sivas-Turkey) for landslide susceptibility mapping by artificial neural Networks,  
443 Bull. Eng. Geol. and the Environ., 68, 297-306, 2009.  
444 Yılmaz, I., Ekemen T., Yıldırım M., Keskin İ., Özdemir G.: Failure and flow development of a collapse induced complex  
445 landslide: the 2005 Kuzulu (Koyulhisar, Turkey) landslide hazard, Environ. Geol., 49, 467-476, 2005.  
446  
447

### NHESS - Figures



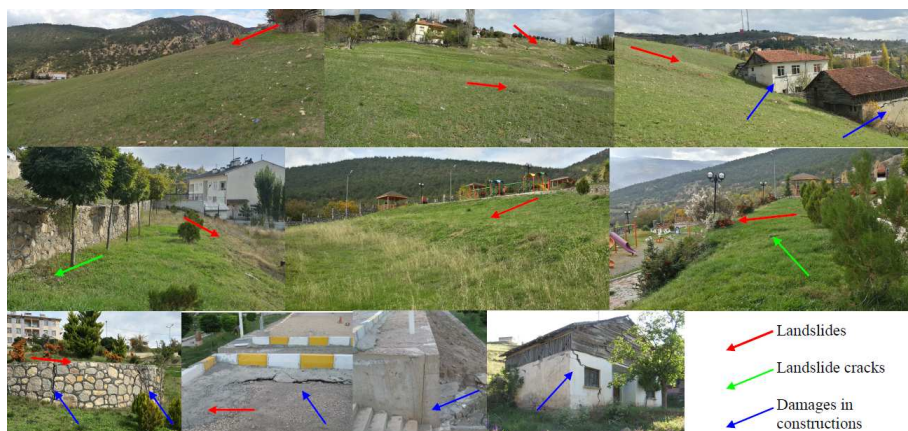
- 448  
449

**Figure 1.** Geological map of study area arranged from Sendir and Yılmaz (2002) and Hastaoğlu (2016).



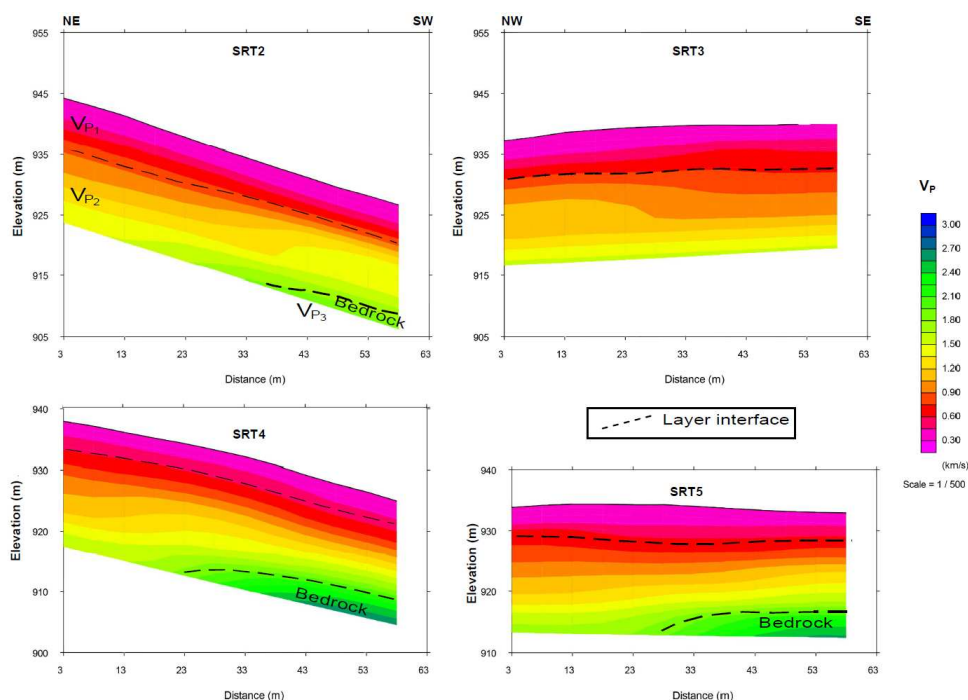
450  
 451  
 452  
 453

**Figure 2.** (a) Geophysics and geodetic data collection locations in the study area. (b), (c) and (d) geophysics profile details.



454  
 455

**Figure 3.** Landslide scene photos (landslide, lanslide cracks and constructional damages).



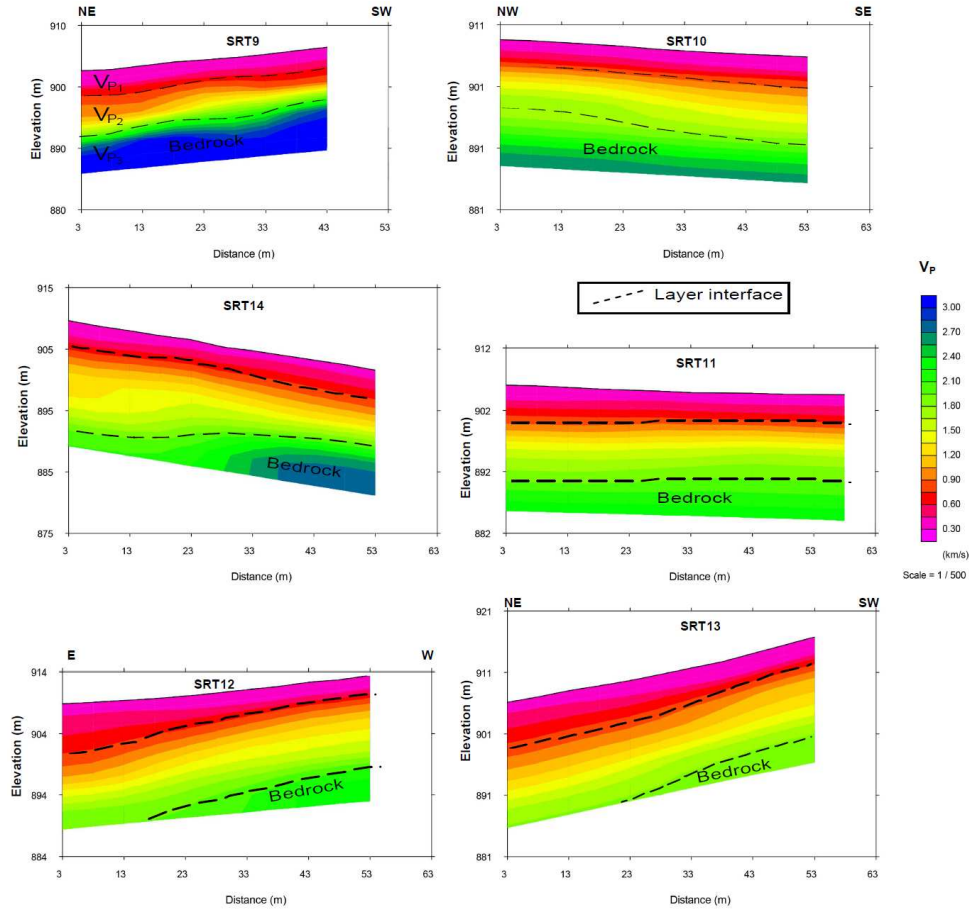
456  
 457 **Figure 4.** The seismic profiles of the area A. The uppermost boundary of the bedrock layer ( $V_{P3}$ ) on the SRT  
 458 images is approximately GPR depth. The lower seismic velocity loose layers (consisting of soil and alluviums, the  
 459 average seismic  $V_{P1}=0.3$  km/s and  $V_{P2}=1.0$  km/s) are on the bedrock (the average seismic  $V_{P3}>2.0$  km/s).  
 460

461  
 462  
 463  
 464  
 465  
 466  
 467  
 468  
 469  
 470  
 471  
 472  
 473



474

475



476

477

478

479

480

481

482

483

484

485

486

**Figure 5.** The seismic profiles of the area C. The uppermost boundary of the bedrock layer ( $V_{P3}$ ) on the SRT images is approximately GPR depth. The lower seismic velocity loose layers (consisting of soil and alluviums, the average seismic  $V_{P1}=0.3$  km/s and  $V_{P2}=1.0$  km/s) are on the bedrock (the average seismic  $V_{P3}>2.0$  km/s).

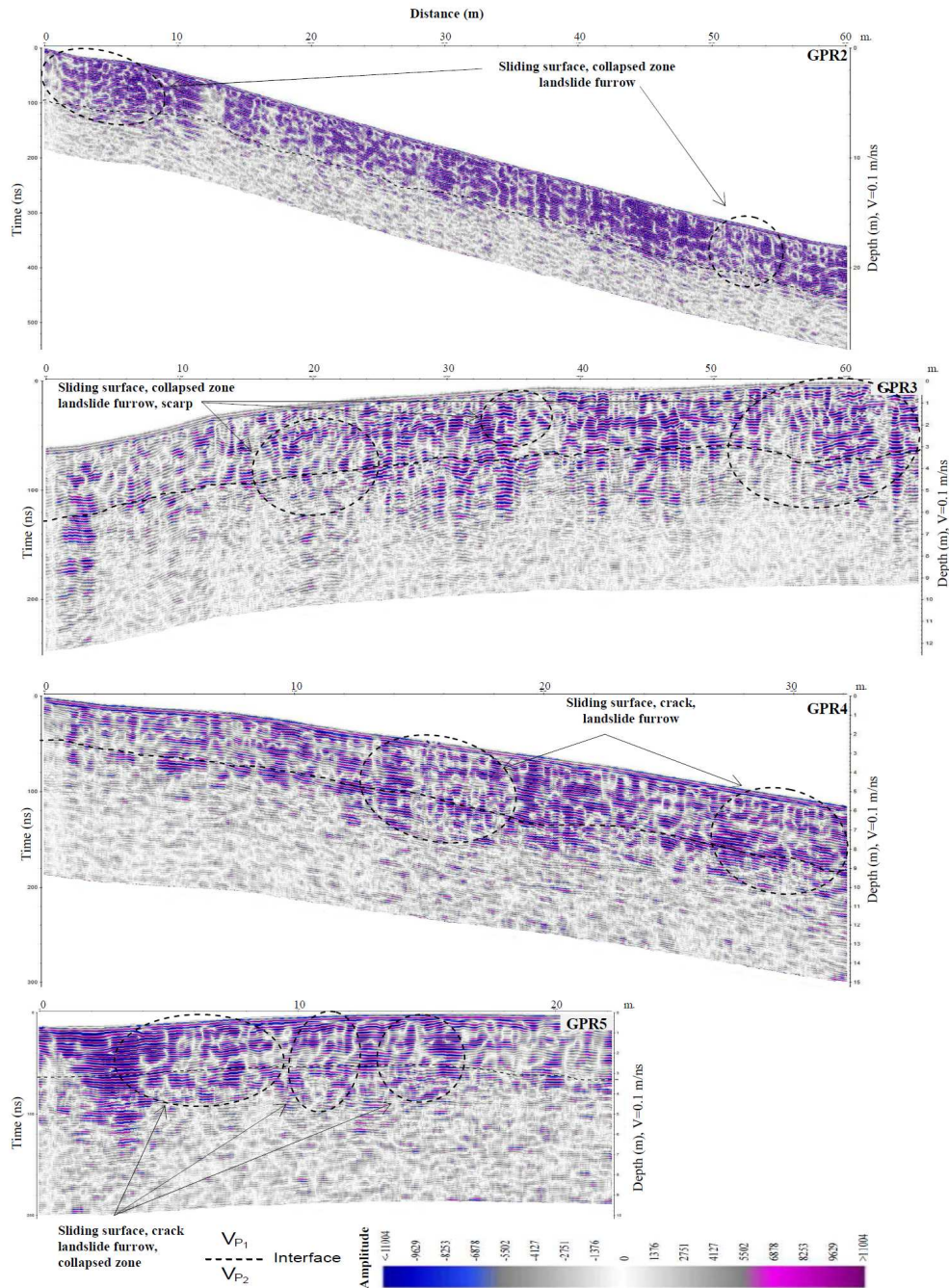
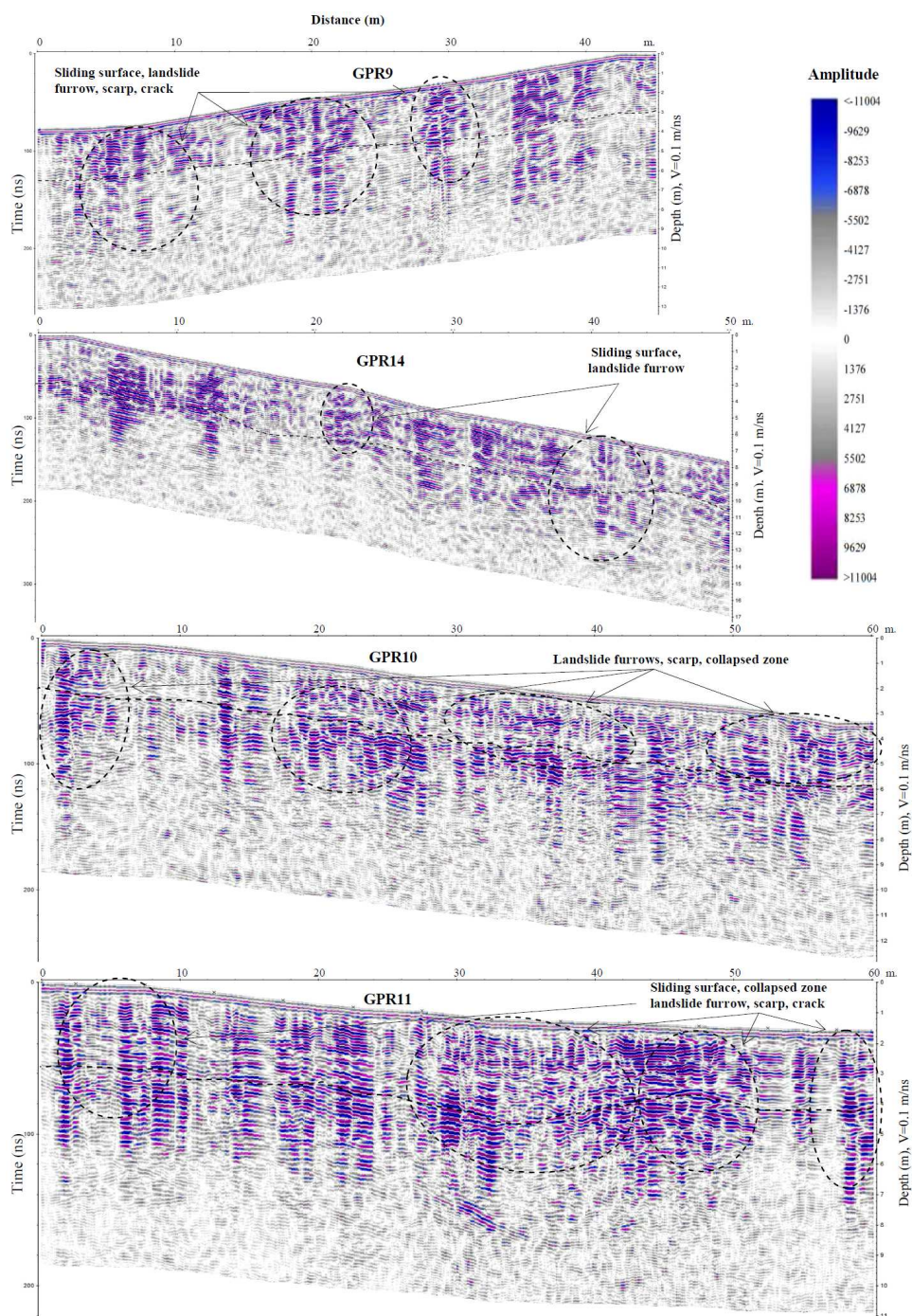


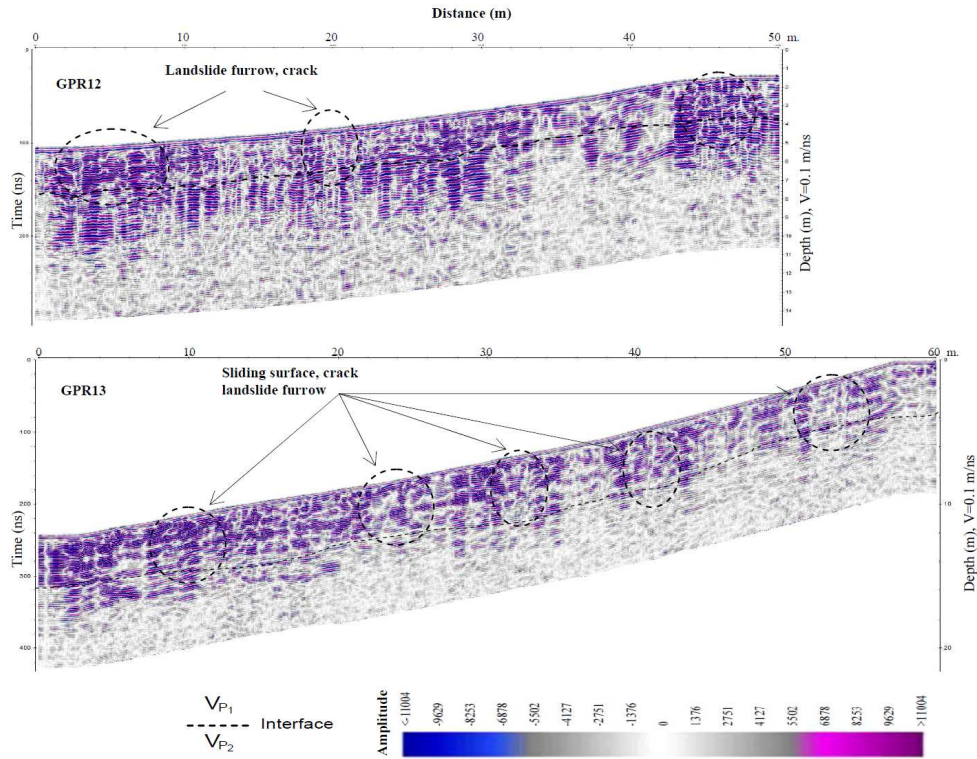
Figure 6. GPR profiles in A area and the deformations in the loose layers (the seismic  $V_{P1}$  and  $V_{P2}$  layers).

487  
 488  
 489  
 490



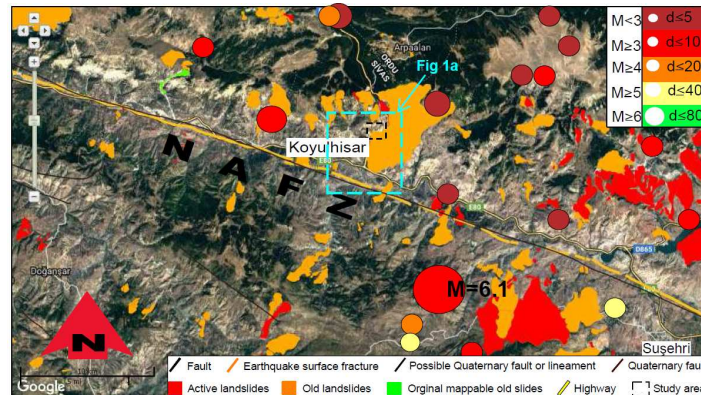
491  
492  
493  
494

**Figure 7.** GPR profiles in the C-west area and the deformations in the loose layers (the seismic  $V_{P1}$  and  $V_{P2}$  layers).



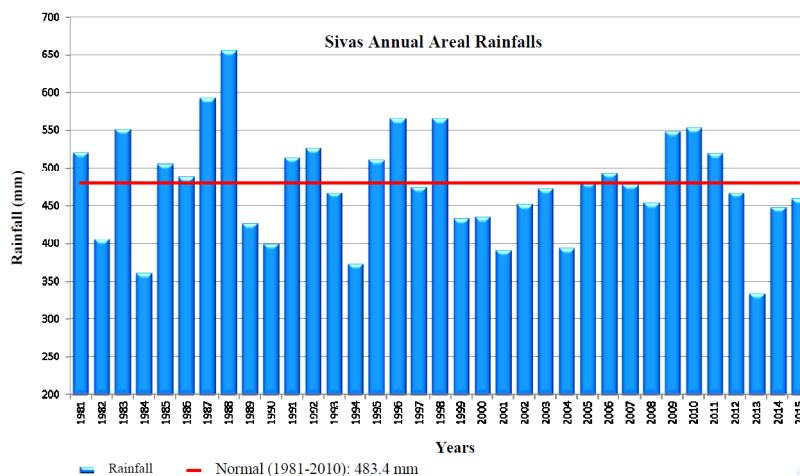
495  
 496  
 497  
 498

**Figure 7. (...contiune)** GPR profiles in the C-east area and the deformations in the loose layers (the seismic  $V_{P1}$  and  $V_{P2}$  layers).



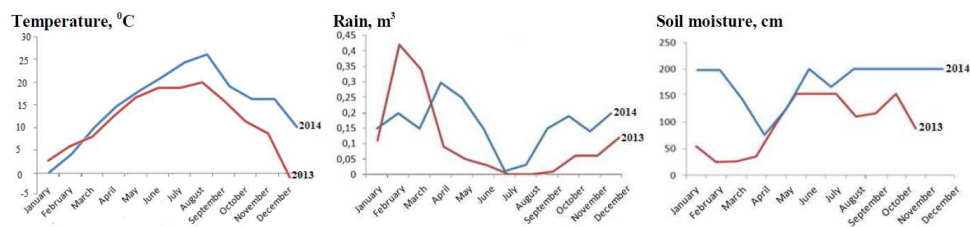
499  
 500  
 501  
 502  
 503  
 504

**Figure 8.** Seismic activity of the study area and its surroundings by the data between 1900-2015 and the landslide areas (UDIM, 2016; MTA, 2018).



505  
 506  
 507

**Figure 9.** Precipitation distribution in between 1981-2015 years of Sivas (MGM, 2016).



508  
 509  
 510  
 511

**Figure 10.** Average monthly temperature ( $T$ ,  $^{\circ}\text{C}$ ), rainfall ( $\text{m}^3$ ) and soil moisture content (cm) change graphics of the study area and its surrounding for 2013-2014. It was prepared from the project data (Hastaoglu et al., 2015).

512  
 513

**Table**

**Table 1.** The annual average meteorological values of Sivas by years between 1950-2015 (MGM, 2016).

SIVAS	January	February	March	April	May	June	July	August	September	October	November	December
The average temperature ( $^{\circ}\text{C}$ )	-3.2	-2.0	2.9	9.1	13.5	17.2	20.2	20.2	16.2	10.8	4.6	-0.6
The average the highest temperature ( $^{\circ}\text{C}$ )	1.0	2.6	8.1	15.3	20.0	24.0	27.9	28.5	24.7	18.4	10.6	3.7
The average the lowest temperature ( $^{\circ}\text{C}$ )	-7.0	-6.2	-1.7	3.4	7.2	9.9	12.0	11.9	8.3	4.4	-0.2	-4.2
The average sunshine duration (hour)	2.3	3.3	4.5	6.2	8.1	10.4	12.1	11.4	9.4	6.3	4.1	2.3
The average number of rainy days	13.0	12.4	13.7	14.0	14.4	8.8	2.5	2.1	4.3	8.0	9.5	12.1
The average monthly total rainfall ( $\text{kg}/\text{m}^2$ )	42.0	40.3	46.0	59.1	60.7	34.8	8.5	5.9	16.9	32.9	41.0	44.2
<b>The highest and the lowest values occurring over many years (1950-2015)</b>												
The highest temperature ( $^{\circ}\text{C}$ )	14.6	18.1	25.2	29.0	32.0	35.5	40.0	39.4	35.7	30.5	22.8	19.4
The lowest temperature ( $^{\circ}\text{C}$ )	-34.6	-34.4	-27.6	-10.9	-4.2	-0.3	3.4	3.2	-3.8	-8.1	-24.4	-27.0
Daily total the highest rainfall	2 May 1991	55.0 $\text{kg}/\text{m}^2$	Daily the fastest wind			5 Jan. 1996	122.8 $\text{km}/\text{h}$	The highest snow		2 Feb. 1950	110.0 cm	

514